

Scale-Resolving Simulation Techniques in Industrial CFD

F.R. Menter¹, J. Schütze, and K. A. Kurbatskii
¹ANSYS Germany GmbH, 83624 Otterfing, Germany

Mikhail Gritskevich and Andrey Garbaruk
NTS St. Petersburg, Russia

The state of Scale-Resolving Simulation (SRS) techniques for turbulent flow predictions in CFD will be reviewed. The emphasis will be on turbulence models which are already in use in industrial simulations. The appropriate application areas for each model group will be discussed.

I. Introduction

WHILE today's CFD simulations are mainly based on RANS models, it is becoming increasingly clear that certain classes of flows are better covered by models, where at least a portion of the turbulence spectrum is resolved in at least a portion of the numerical domain. Such methods are termed Scale-Resolving Simulation (SRS) models here.

RANS models have shown their strength essentially for wall-bounded flows, where the calibration according to the law-of-the-wall provides a sound foundation for further refinement. For free shear flows, the performance of RANS models is much less uniform. There is a wide variety of such flows, ranging from simple self-similar flows like jets, mixing layers and wakes, to impinging flows, flows with strong swirl, massively separated flows and many more. Considering that RANS models typically already have limitations covering the most basic self-similar free shear flows with one set of constants, there is little hope that even the most advanced Reynolds Stress Models (RSM) will eventually be able to provide a reliable foundation for all such flows. On the other hand, for free shear flows, it is typically much easier to resolve the largest turbulent scales, as they are of the order of the thickness of the shear layer. In contrast, for wall boundary layers, the turbulence length scale becomes very small relative to the boundary layer thickness near the wall (increasingly so with increased Re number). This poses severe limitations for Large Eddy Simulation (LES) models as the computational effort required is still far from the computing power available to industry. For this reason, hybrid models are under development, where large eddies are only resolved away from walls and the wall boundary layers are covered by a RANS model (e.g. Detached Eddy Simulation – DES or Scale-Adaptive Simulation – SAS). A further step is the application of a RANS model only in the innermost part of the wall boundary layer and then to switch to an LES model for the main part of the boundary layer. Such models are termed Wall Modelled LES (WMLLES). Finally, for large domains, it is frequently only necessary to cover a small portion with SRS models, while the majority of the flow can be computed in RANS mode. In such situations, zonal or embedded LES methods are attractive. Such methods are typically not new models in the strict sense, but allow the combination of existing models/technologies in a flexible way in different portions of the flowfield. Important elements of zonal models are interface conditions, which convert turbulence from RANS mode to resolved mode at pre-defined locations. In most cases, this is achieved by introducing synthetic turbulence based on the length and time scales from the RANS model.

There is a large variety of hybrid RANS-LES models with often somewhat confusing naming conventions concerning the range of turbulence eddies they will resolve. On close inspection, many of these models are slight variations of the Detached Eddy Simulation (DES) concept of Spalart with a very similar performance. The present paper will provide a review of models which are in, or at the verge of, industrial use – which reduces the model variety considerably. Naturally, the authors will focus on the methods employed in our CFD codes, and more specifically ANSYS-Fluent. For a general overview of SRS modelling concepts see e.g. Fröhlich and von Terzi (2008).

II. Large Eddy Simulation - LES

Large Eddy Simulation (LES) has been the first SRS method and is under development for almost five decades starting from the early work of Smagorinsky (1963). LES has in all this time never lived up to the expectations that it could eventually replace RANS models on a grand scale, despite the substantial effort invested into this technology. The main limitation originates from the high resolution demands for wall-bounded flows. For this reason, classical LES has largely remained a research tool, with some sporadic industrial applications to flows not much affected by wall boundary layers, like free shear flows or flows with very limited regions of wall boundary layers.

It is instructive to compare the numerical effort required for a RANS and a LES simulation for the flow over a relatively limited geometry, like a single turbine blade in a gas turbine at a Reynolds number of $Re \sim 10^5$ (see e.g. Michelassi et al. 2003). If all physical effects like laminar-turbulent transition and the complete 3D geometry with hub and shroud portions are included the estimates are given in Table 1:

	Number of cells	Number of time steps	Number of inner loops per time step	Effort relative to RANS
RANS	$\sim 10^6$	$\sim 10^2 - 10^3$	1	1
LES	$\sim 10^8 - 10^9$	$\sim 10^5$	1-10	$\sim 10^5 - 10^6$

Table 1: Estimate of CPU resources for RANS and wall-resolved LES for a single turbine blade

Of course, details depend on numerics and code specifics etc., but the estimate shows that routine application of LES for industrial, wall-bounded flows is out of reach for several decades, even for relatively simple geometries and moderate Reynolds numbers. One could argue that this is an extreme case as laminar-turbulent transition needs to be resolved, however, estimates at higher Re numbers as provided by Spalart (1997, 2000) are not more favorable. For this reason, pure LES will not become a standard industrial tool for most applications for several decades.

III. Detached Eddy Simulation - DES

Detached Eddy Simulation (DES) has been proposed by Spalart and co-workers (Spalart 2000, Spalart et al. 2006, Strelets 2001), to eliminate the main limitation of LES models, by proposing a hybrid formulation which switches between RANS and LES based on the grid resolution provided. By this formulation, the wall boundary layers are entirely covered by the RANS model and the free shear flow portions are typically computed in LES mode. The formulation is mathematically relatively simple and can be built on top of any RANS turbulence model. DES has attained significant attention in the turbulence community as it allows the inclusion of SRS capabilities into every day engineering flow simulations.

Within the DES model, the switch between RANS and LES is based on a criterion like:

$$C_{DES} \Delta > L_t \rightarrow RANS \quad ; \quad \Delta = \max(\Delta_x, \Delta_y, \Delta_z)$$

$$C_{DES} \Delta \leq L_t \rightarrow LES$$

It is also important to realize that resolved turbulence is not explicitly introduced into the simulation by an explicit conversion of modeled turbulence to resolved turbulence. The method relies on a sufficiently strong flow instability (e.g. as observed behind bluff bodies) to produce the resolved content by itself. Obviously, such instability is not always present and switching the model might simply result in a reduction of the RANS Eddy-Viscosity to an LES formulation without a proper generation of turbulent content. This is the case for wall boundary layers. If the grid is reduced to activate the DES-limiter, the eddy-viscosity is reduced and the RANS model is no longer functional. In many situations this can lead to Grid-Induced Separation (GIS) (Menter and Kuntz, 2002) where the boundary layers separates at arbitrary locations based on the grid spacing. In order to avoid this limitation, the DES concept has been extended to Delayed-DES (DDES), following the proposal of Menter and Kuntz (2002) to ‘shield’ the boundary layer from the DES limiter (Shur et al. 2008). Using DDES is now the recommended practice. The effectiveness depends on the details of the shielding function. Functions which provide ‘high’ protection against

GIS can in turn limit the models LES capabilities. This is especially true for internal flows, where the domain of interest is surrounded by multiple walls and the model can frequently not distinguish between attached and detached regions. DDES is therefore most suitable for external aerodynamic flows.

Another important issue to understand is that also for free shear flows (where shielding is not active), the DES limiter is activated much before the grid is actually able to resolve the flow with LES-quality. There is approximately an order of magnitude in grid spacing between the activation of the limiter and a sufficient LES resolution. Grids falling in-between these limits produce ‘grey zones’, meaning zones where the flow is neither in RANS nor in LES mode. The user of any DES model needs to be keenly aware of such limitations and needs to very carefully craft an appropriate numerical mesh to avoid undefined model behavior. Independent of this technical details, (D)DES is the most frequently applied hybrid RANS-LES model in industrial CFD simulations. It also has prompted a substantial number of developments in the area of hybrid RANS-LES models, and has put SRS within reach of engineers. Successful applications of the DES model can be found in (Spalart 2000, Spalart et al. 2006, Strelets 2001, Shur, 2008, Haase et al., 2009).

IV. Scale-Adaptive Simulation – SAS

In recent years, the author’s group has developed an alternative method to DES, for which the RANS model is not influenced by the grid spacing (Menter et al. 2010, Egorov et al. 2010). The method is termed Scale-Adaptive Simulation (SAS) and is based on the introduction of the von Karman length scale, L_{vK} , into the turbulence model:

$$L_{vK} = \kappa \left| \frac{U'}{U''} \right|; \quad |U'| = \sqrt{\frac{\partial U_i}{\partial x_j} \frac{\partial U_i}{\partial x_j}}; \quad |U''| = \sqrt{\frac{\partial^2 U_i}{\partial x_k^2} \frac{\partial^2 U_i}{\partial x_j^2}}$$

Unlike DES, SAS models are not affected by GIS or grey zones and can be run on a much wider range of numerical grids. L_{vK} , allows the model to adjust to resolved structures in the simulation and automatically reduces the eddy-viscosity in such regions to the appropriate LES level if the grid permits. However, if the grid is not of LES resolution, SAS will still produce sensible results, and under coarse meshes and or large time steps will fall back to the RANS solution. Like the DES mode, the SAS model also relies on an instability of the flow to generate resolved turbulence. In case such an instability is not present, the model will remain in RANS mode.

Figure 1 shows the flow structures computed by the SST-SAS model for a periodic hill flow. The two pictures represent simulations on the same mesh (~2.5 million nodes) using 2 different time steps. The time step in the left part of the figure corresponds to a typical LES time step (CFL<1), in the right part the time step is increased by a factor of four. Further increasing the time step would result in a steady state RANS solution. Figure 1 illustrates the terminology Scale-Adaptive, which allows the model to adjust to the mesh and time step resolution provided, resulting in a continuous variation of the simulation from LES to steady-state RANS. The color in the Figure 1 displays the ratio of eddy-viscosity to molecular viscosity. In the left part of Figure 1 this ratio is of order 5-10 and in the right part of order 30-50. The ability of the model to adjust its eddy-viscosity to the resolved scales is unique and cannot be achieved with standard LES models. For Smagorinsky type models ($\nu_t=(c\Delta)^2S$), the length scale is fixed by the grid spacing, Δ . For large scales, the strain rate, S , is lower than for small scales. Such a model would therefore produce a lower eddy-viscosity for large structures than for small ones.

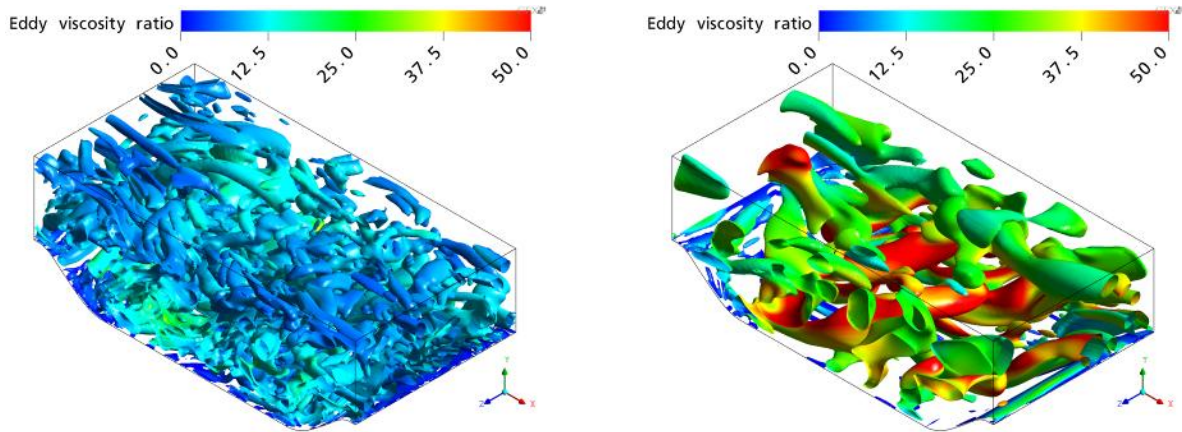


Figure 1: Turbulent structures for flow over periodic hill with SST-SAS model. Left: Small time step (CFL~1), Right 4x larger time step. Color: ratio of eddy-viscosity to molecular viscosity.

Figure 2 shows the velocity profiles computed with the SAS model using the two different time steps in comparison with the reference LES (Temmerman and Leschziner, 2001) and the SST-RANS solution. It can be seen that even the large time step leading to the structures seen in the right side of Figure 1 gives a significant improvement in the velocity profiles compared to the steady state solution (this case is known to be challenging for RANS models due to its large separation zone and periodic conditions).

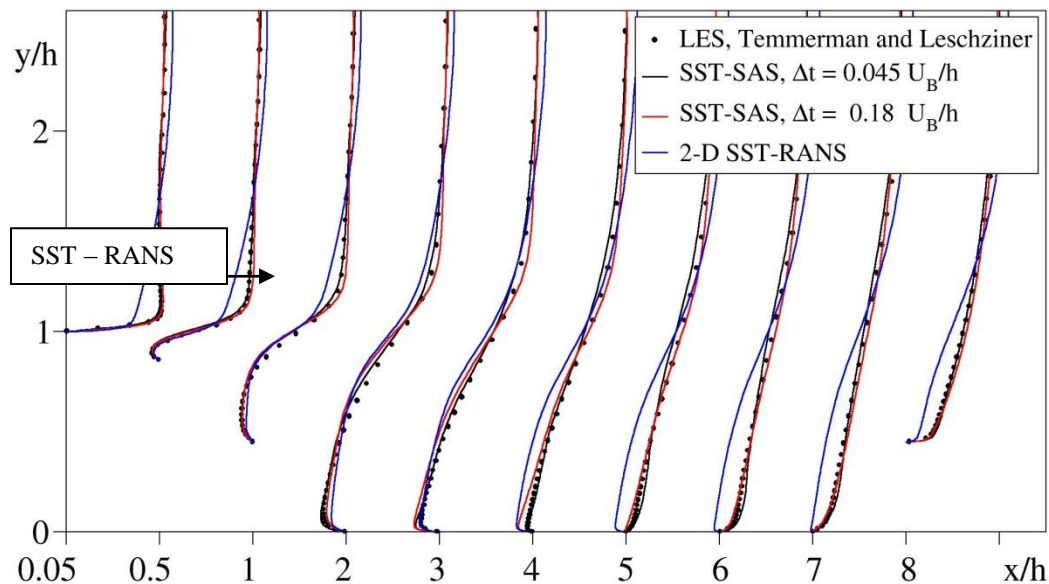


Figure 2: Velocity profiles for the SAS simulations with different time steps for periodic hill flow in comparison with reference LES and SST-RANS solution

Figure 3 shows SAS simulations over a generic airplane geometry (Laschka et al. ,1995). The simulation ($Re=2.8 \times 10^6$, $\alpha=15^\circ$) has been carried out on an unstructured mesh with 11×10^6 control volumes. The left part shows the geometry and the turbulent structures produced by the simulation. The right part shows a comparison between the experimental data and the time averaged simulation. The simulation is in good agreement with the exp. data (right part of figure).

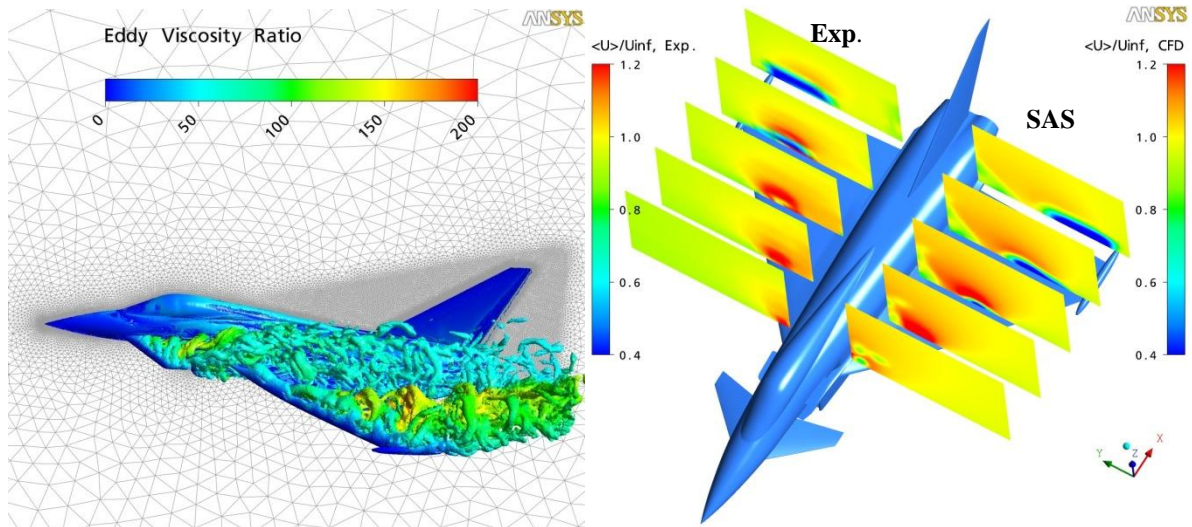


Figure 3: Flow over generic airplane configuration FA-5. Left - flow structures. Right - comparison of exp. and SAS axial flow component. (Geometry and data are Courtesy of EADS Deutschland)

Air flow past a 3-D rectangular shallow cavity was calculated in order to test the SAS models ability to predict correct spectral information for acoustics applications. The cavity geometry and flow conditions corresponding to the M219 experimental test case of Henshaw (2000). The experiment investigates the noise generation due to turbulent structures forming from the front lip of the cavity and interacting with the cavity walls.

Figure 4 shows the turbulent structures, produced by the SST-SAS model (iso-surface Q-criterion). The power spectral density (PSD) of the transient pressure signals calculated and measured by sensors on the cavity bottom near the leading and the downstream wall respectively is plotted in Figure 5. These plots show that the PSD levels are captured in good agreement with the data. Similar agreement was achieved for the other experimental locations (not shown here) Kurbatskii et al (2011).

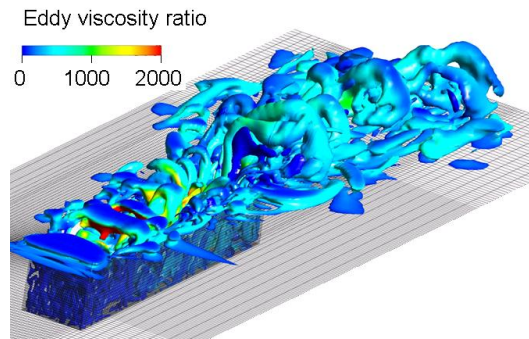


Figure 4: Resolved turbulent structures for cavity flow: iso-surface $\Omega_2-S_2=5 \cdot 10^5 \text{ s}^{-2}$.

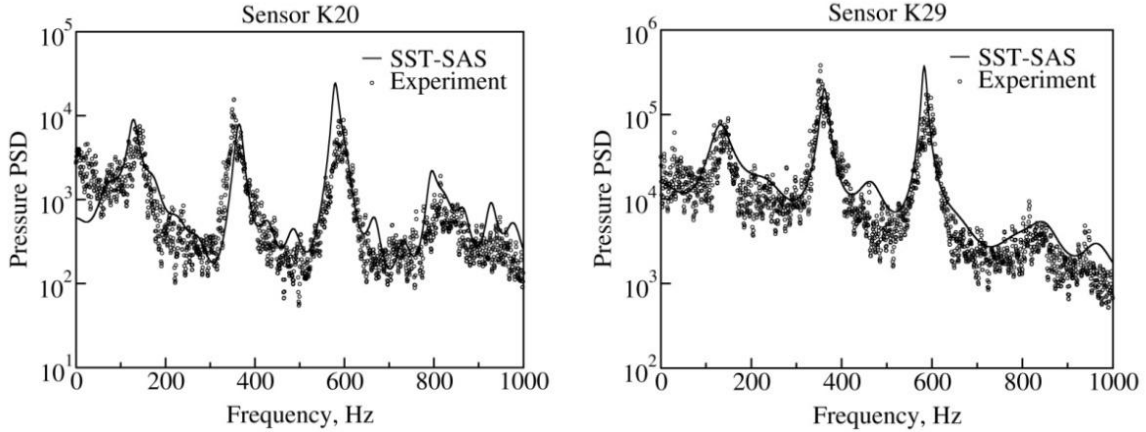


Figure 5: Power spectral density of the transient wall pressure signals on the cavity bottom: left – sensor K20 located close the front wall, right – sensor K29 located close to the rear wall.

In Egorov et al. (2010) the SAS model is described in detail and is applied to a wide variety of generic and industrial-like flows.

V. Wall Modelled Large Eddy Simulation - WMLES

A relatively recent approach to address the LES-limitations for high RE number boundary layers is termed Wall-Modelled LES (WMLES). It is based on the concept of covering the inner portion of the boundary layer by a RANS and the outer portion by a LES formulation (Nikitin et al. 2000). This avoids the very high resolution requirements of LES in the inner wall layer. A very simple and promising approach to WMLES has been proposed by Shur et al. (2008). It is based on a reformulation of the length scale used in the LES zone and by blending it with the mixing length (RANS) model in the inner part of the boundary layer. The formulation of Shur et al. is given by:

$$\nu_t = \min \left[\kappa d_w^2, C_{SMAG} \Delta^2 \left(1 - \exp \left[- y^+ / 25^3 \right] \right) S \right]$$

$$\Delta = \min \left[\max \left(C_w d_w, C_w h_{max}, h_{wn}, h_{max} \right), C_w \approx 0.15 \right]$$

where d_w is the wall distance, S is the shear strain rate, h_{max} is the largest edge length of the current computational cell and h_{wn} is the cell size in wall normal direction. This model was calibrated for a 4th order central difference scheme, and needs to be lightly adjusted for lower order schemes.

Figure 6 shows a series of simulations for periodic channel flows with increasing Reynolds number using ANSYS-Fluent 13. The grids used for these simulations are given in Table 2. It is well known that the use of hybrid models like DES can result in a strong log-layer mismatch and a corresponding error in the wall shear stress (Spalart et al., 2006) when applied as a WMLES model. Figure 6 shows that the log-layer miss-match can be reduced to a relatively small shift at the RANS-LES interface, resulting in a high quality solution even at very high Re numbers for the above formulation (see also Shur et al. (2008)).

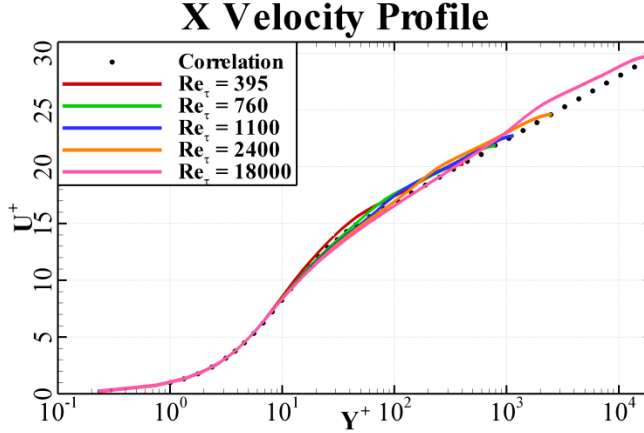


Figure 6: Velocity profiles in logarithmic scale for periodic channel flow using WMLES for various Reynolds numbers.

The simulations were carried out on grids with the characteristics given in Table 2. The domain size was $LX=16h$, $LY=2h$, $LZ=3h$ (h being half the channel height – this corresponds approximately to the boundary layer thickness for wall boundary layers). The main characteristics of WMLES is clearly visible from Table 2, the non-dimensional values for $\Delta X+$ and $\Delta Z+$ are far beyond the limits of standard LES methods ($\Delta X+=40$, $\Delta Z+=20$). For WMLES, one only has to ensure a minimum number of cells per boundary layer volume $\delta x \delta y \delta z$. In the current formulation the minimum resolution per boundary layer volume is of the order of $10 \times 40 \times 20$ cells (streamwise, normal and spanwise).

Re_τ	Cells Number	Nodes Number	$\Delta X+$	$\Delta Y+$	$\Delta Z+$
395	384 000	$81 \times 81 \times 61$	40.0	$0.2 \div 30$	20.0
395	1 764 000	$141 \times 141 \times 91$	26.6	$0.2 \div 20$	13.3
760	480 000	$81 \times 101 \times 61$	76.9	$0.2 \div 30$	38.5
1100	480 000	$81 \times 101 \times 61$	$111. \div 4$	$0.2 \div 30$	55.7
2400	528 000	$81 \times 111 \times 61$	$243. \div 0$	$0.2 \div 30$	$121. \div 5$
18000	624 000	$81 \times 131 \times 61$	$1822. \div .7$	$0.2 \div 30$	$911. \div 4$

Table 2: Grids for periodic channel flow at different Reynolds number using WMLES

The grid for Boundary Layer test case has the parameters given in Table 3.

Re_Θ	Cells Number	Nodes Number	$\Delta X+$	$\Delta Y+$	$\Delta Z+$
1000/10000	1 050 000	$251 \times 71 \times 62$	16	$0.2 \div 80$	8

Table 3: Grids for boundary layer flow at different Reynolds number using WMLES

Figure 7 shows the turbulent structures for a wall boundary layer flow using the WMLES option. Again the outer part is covered by LES and the near wall part by RANS. The flow is also computed with ANSYS-Fluent 13 and the turbulence at the inlet is generated by the Vortex Method (Mathey et al. 2006). The turbulence is well maintained as can be seen from Figure 7. In Figure 8 the wall shear stress is displayed. The WMLES recovers quickly from the synthetic turbulence and maintains a proper wall shear stress downstream.

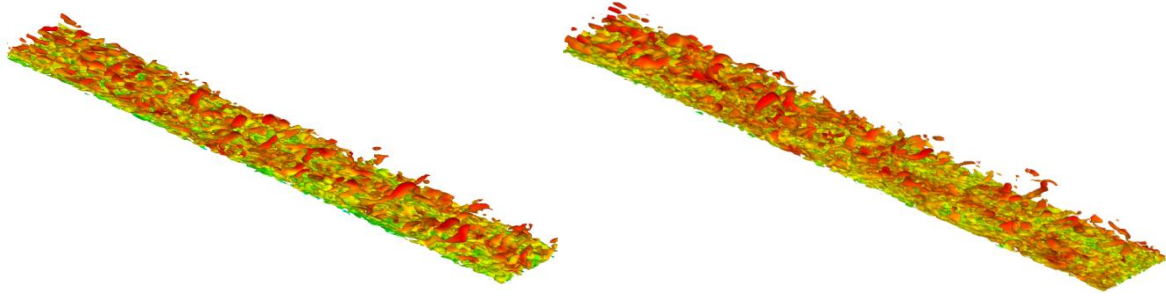


Figure 7: Turbulence structures for wall boundary layer flow using the WMLES option and the vortex method to generate synthetic turbulence at the inlet. Right $Re_\theta=1000$, Left $Re_\theta=10000$.

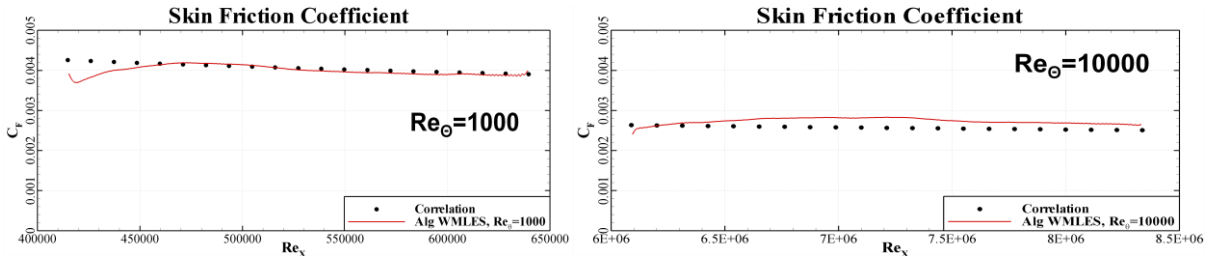


Figure 8: Wall shear stress coefficient for wall boundary layer flow using the WMLES option and the vortex method to generate synthetic turbulence at the inlet. Right $Re_\theta=1000$, Left $Re_\theta=10000$.

It should be noted that WMLES is still substantially more computationally expensive than RANS. However, it avoids the excessive Re number scaling of classical wall-resolved LES and allows the simulation of limited components of technical devices at high Reynolds numbers for which RANS model simulations are not of sufficient accuracy.

VI. Embedded LES - ELES

As pointed out in the previous sections, hybrid models like DES and SAS rely on flow instabilities to generate turbulent structures in large separated regions without the explicit introduction of unsteadiness through the boundary conditions. However, there are situations, where such instabilities are not present or are not reliable to serve this purpose. In such cases, it is desirable to apply RANS and the LES models in predefined zones and provide clearly defined interfaces between them. At these interfaces, the modeled turbulent kinetic energy from the upstream RANS model is converted explicitly to resolved scales at an internal boundary to the LES zone. The LES zone can then be limited to the region of interest where unsteady results are required.

There are numerous zonal RANS-LES concepts, and it is not possible to cover all of them. The following results are therefore limited to the method implemented in ANSYS-Fluent 13. This approach has been selected as it appears attractive from an industrial CFD perspective (Cokljat et al. 2009). It allows the user to pre-specify RANS and LES zones in a single CFD simulation. At the RANS-LES interface, the modeled turbulence from the RANS model is converted into resolved turbulence using the methods previously available for this purpose at inlets. ELES allows the selection of virtually all RANS models in the RANS domain and all algebraic LES models in the LES region.

Figure 9 shows the application of ELES to a channel flow. The front portion of the channel is covered by the SST RANS model (Menter, 1994). The RANS-LES interface uses the Vortex Method (Mathey et al. 2006) to convert modeled turbulence to resolved synthetic turbulence and the WALE LES (Nicoud and Ducros, 1999) model to provide an LES eddy-viscosity. Downstream, the method switches back to RANS. The numerical method allows switching from Second Order Upwind to Central Difference between the RANS and the LES region. An alternative is to use a Bounded Central Difference (BCD) (Jasak et al. 1998) scheme in the entire domain.

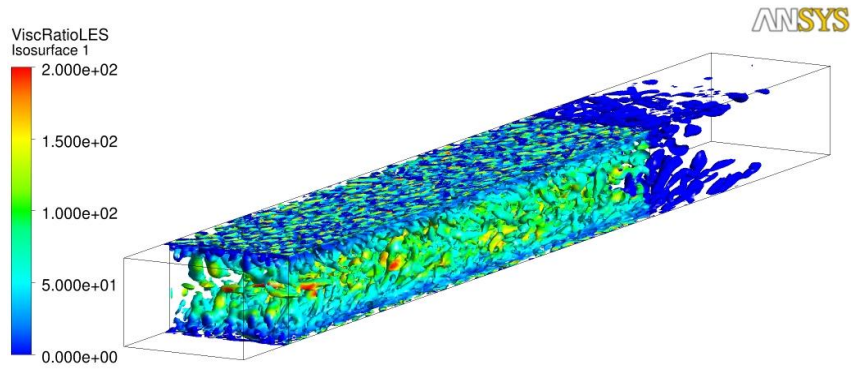


Figure 9: Channel flow. Viscosity ratio on iso-surfaces of Q-criterion (-500).

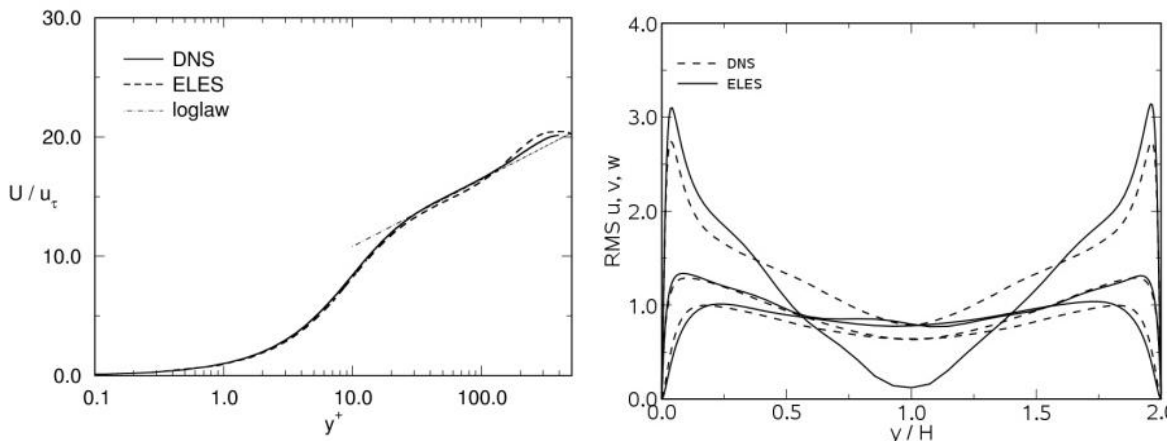


Figure 10: Fully developed channel flow. Mean velocity values inside LES zone (left), rms values inside LES zone at $x = 1.5 + 1.5\pi$ (right).

Figure 10 shows a comparison of the LES results inside the embedded region with DNS data of (Moser et al., 1998), both for the mean flow profile and the turbulence RMS values. The agreement is quite close, considering the limited length of the LES zone.

A more challenging test case for ELES in combination with WMLES has been computed within the EU project ATAAC. It is the flow over a hump with a relatively large separation zone on the leeward side. Figure 11 shows the experimental set-up (Greenblatt et al. 2005).

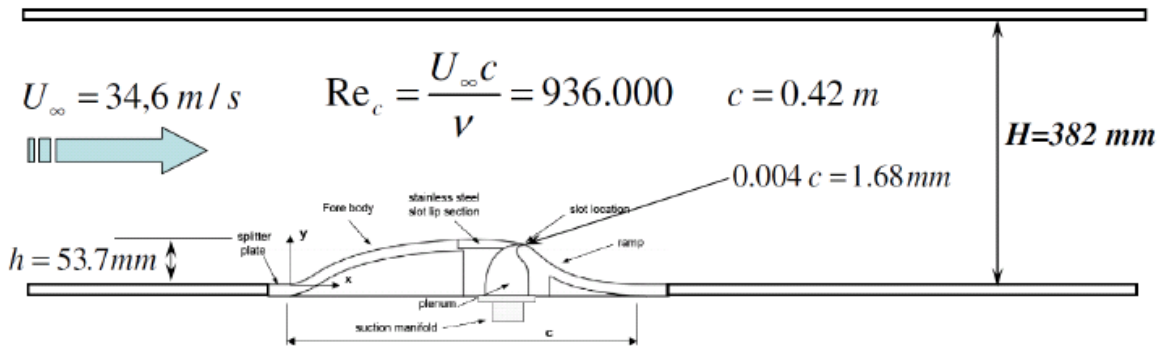


Figure 11: Experimental setup up for NASA hump flow experiment

The flow has been computed with ANSYS-Fluent 13.0 using the SST model in the RANS zone, the vortex method at the RANS-LES interface and the WMLES option in the LES zone.

The grid for the testcase can be seen in Figure 12 together with a visualization of the turbulent structures in the LES zone. The grid in the LRS zone consists of $200 \times 100 \times 100$ cells and is designed to provide $10 \times 40 \times 20$ cells in streamwise, normal and spanwise direction per boundary layer volume. The RANS grid is much coarser, especially in the spanwise direction. It should be noted that the momentum thickness Reynolds number at the inlet to the LES domain is relatively high ($Re_\theta = 7000$).

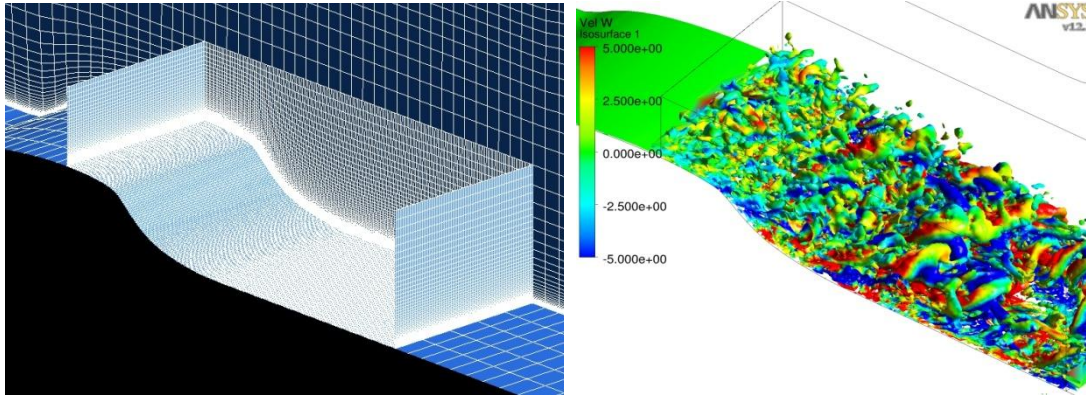


Figure 12: Left: grid for the NASA hump simulation. Right: turbulent structures in the LES domain (colour spanwise velocity component).

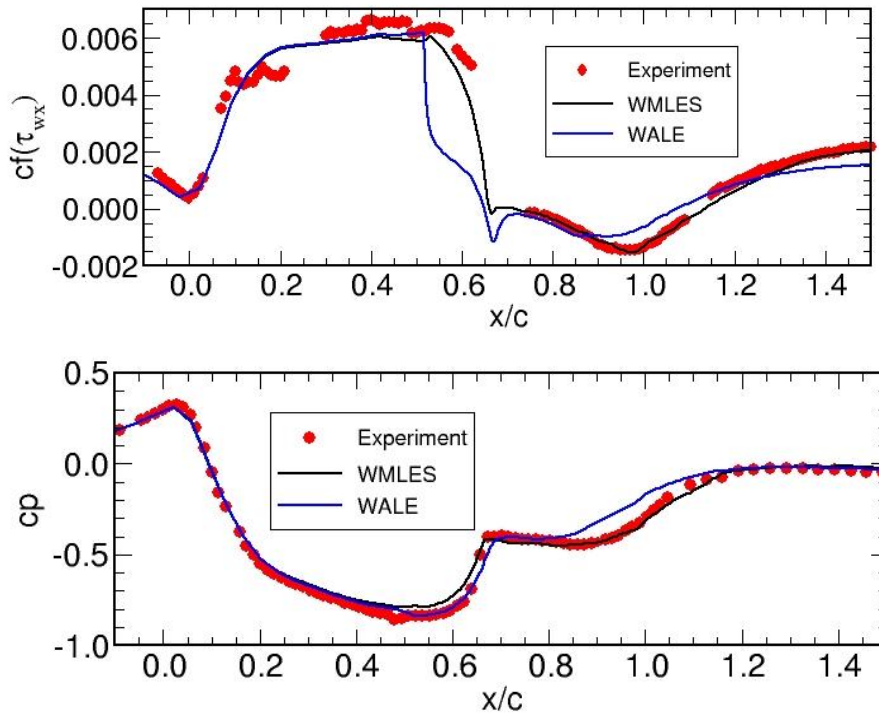


Figure 13: Wall shear stress, cf , and wall pressure coefficients, cp , for NASA hump flow simulations. Comparison of WMLES and WALE LES method in the LES domain.

Figure 13 shows the wall shear stress and the wall pressure coefficient for these simulations. It can be seen that the combination with the WMLES formulation provides a close agreement even with the very sensitive wall shear stress coefficient, cf . From the pressure coefficient, cp , it can also be seen that the length of the separation zone is predicted correctly. One of the more interesting observations from the study resulted from the application of the standard WALE LES model inside the LES zone. Due to the high Re number, the WALE model is not able to carry

the turbulent boundary layer. It separates immediately after the RANS-LES interface and overpredicts the separation length. This clearly illustrates the advantages of WMLES for higher Re number wall bounded flows.

VII. Summary

Turbulence modelling is and will remain one of the driving technologies in CFD. The wide range of applications of industrial CFD codes demands a balanced model offering, which allows the inclusion of all relevant physical effects while providing solutions with available computing power and within acceptable turn-around times for industrial users. For many applications, RANS models are and will remain the optimal choice in terms of a proper balance of accuracy and computational resources.

The main thrust in industrial CFD turbulence modelling in the next decades will be in the area of Scale-Resolving Simulation (SRS) models. Industrial CFD codes will have to offer a wide range of the most advanced model formulations, ranging from SAS, DES all the way to zonal methods with interface conditions. Finally, the challenge of computing high Re number flows with Wall-Modelled LES will continue to be a focal point of future research activities.

Acknowledgments

Part of this work was carried out under the EU project ATAAC (Advanced Turbulence Simulation for Aerodynamic Application Challenges) funded by the European Community in the 7th Framework Programme under Contract No. ACP8-GA-2009-233710-ATAAC.

References

Cokljat D., Caradi D., Link G., Lechner R. and Menter F.R., (2009), "Embedded LES Methodology for General-Purpose CFD Solvers". Proc. Turbulent Shear Flow Phenomena, Proc. 6th Int. Symp. Turbulence and Shear Flow Phenomena, Seoul, Korea, 22-24 June 2009, 1191-1196.

Egorov Y., Menter F.R. and Cokljat D., (2009), "Scale-Adaptive Simulation Method for Unsteady Flow Predictions. Part 2: Application to Aerodynamic Flows", Journal Flow Turbulence and Combustion, Vol. 85, No. 1, pp. 139-165.

Fröhlich J. and von Terzi D. (2008), "Hybrid LES/RANS methods for simulation of turbulent flows", Progress in Aerospace Sciences, Vol. 44, Issue 5, pp 349-377, 2008.

Greenblatt D., Paschal K. B., Yao C.-S. and Harris J. (2005): "A Separation Control CFD Validation Test Case, Part 2: Zero Efflux Oscillatory Blowing". AIAA Paper No. 2005-0485 (also in AIAA Journal, Vol. 44, No. 12, 2006, pp. 2831-2845).

Haase W., Braza M. and Revell A., (2009), "DESider – A European Effort on Hybrid RANS-LES Modelling", Notes on Numerical Fluid Mechanics and Multidisciplinary Design, Vol. 103, Springer.

Henshaw M. J. de C. (2000): "M219 cavity case, In: "Verification and validation data for computational unsteady aerodynamics", Tech. Rep. RTO-TR-26, AC/323/(AVT) TP/19, pp. 473-480.

Jasak H, Weller H.G. and Gosman A.D., "High Resolution Differencing Scheme for Arbitrarily Unstructured Meshes", Int. J. Numer. Meth. Fluids, 1999, v31, pp 431-449.

Kurbatskii, K. A., Menter, F., Schuetze, J., and Fujii, A. (2011), "Numerical Simulation of Transonic Cavity Noise using Scale-Adaptive Simulation (SAS) Turbulence Model," Inter-Noise 2011, September 2011.

Laschka B., Ranke and H., Breitsamter C., (1995): "Application of unsteady measurement techniques to vortical and separated flows", Z. Flugwiss. Weltraumforsch. 19, 90-108.

Mathey F., Cokljat D., Bertoglio J.P. and Sergent E. (2006), "Specification of LES Inlet Boundary Condition Using Vortex Method", Progress in Computational Fluid Dynamics, Vol. 6, No 1-3, pp. 58--67.

Menter F.R. and Kuntz M., (2002), "Adaptation of Eddy-Viscosity Turbulence Models to Unsteady Separated Flow behind Vehicles". Proc. Conf. The Aerodynamics of Heavy Vehicles: Trucks, Busses and Trains, Asilomar, Ca, 2002.

Menter, F.R., (1994), "Two-Equation Eddy-Viscosity Turbulence Models for Engineering Applications", AIAA-Journal, 32(8), pp. 269-289, 1994

Menter F.R. and Egorov Y., (2010), "Scale-Adaptive Simulation Method for Unsteady Flow Predictions. Part 1: Theory and Model Description", Journal Flow Turbulence and Combustion, Vol. 85, No. 1, pp 113-138.

Michelassi V., Wissink, J. G. and Rodi W. (2003), "Direct numerical simulation, large eddy simulation and unsteady Reynolds-averaged Navier-Stokes simulations of periodic unsteady flow in a low-pressure turbine cascade: A comparison", Journal of Power and Engineering. Vol 217, Number 4, pp. 403-411.

Moser R.D., Kim J. And Mansour N.N., (1998), "DNS of turbulent channel flow up to $Re_{\tau}=590$ ", Phys. Fluids, Vol11, pp. 943-945.

Nicoud, F. and Ducros, F.: Subgrid-scale stress modelling based on the square of the velocity gradient tensor. Flow, Turb. Combust. 62, 183-200, (1999).

Nikitin N., Nicoud, F. Wasistho B., Squires K., and Spalart P.(2000), "An approach to wall modeling in large-eddy simulations". Phys. Fluids, 12(7):1629–1632, 2000.

Shur, M.L., Spalart P.R., Strelets M. and Travin A., (2008), "A hybrid RANS-LES approach with delayed-DES and wall-modelled LES capabilities". Int. J. Heat Fluid Flow International Journal of Heat and Fluid Flow, Vol. 29, No 6, pp. 1638-1649.

Smagorinsky, J. (1963), "General Circulation Experiments with the Primitive Equations, I. the Basic Experiment". Monthly Weather Review, 91(3): pp 99-164, 1963.

Spalart, P.R., Jou, W., Strelets, M., Allmaras, S. (1997), "Comments on the feasibility of LES for wings, and on a hybrid RANS/LES approach". In: Advances in DNS/LES, 1st AFOSR Int. Conf. on DNS/LES,.

Spalart P. R. (2000), "Strategies for turbulence modelling and simulations", Int. J. Heat Fluid Flow, 21, pp. 2.

Strelets, M. (2001), "Detached Eddy Simulation of massively separated flows". AIAA Paper 2001-879.

Spalart, P., Deck, S., Shur, M., Squires, K., Strelets, M., Travin, A., (2006), "A New Version of Detached Eddy Simulation, Resistant to Ambiguous Grid Densities", Journal of Theoretical and Computational Fluid Dynamics 20, pp. 181–195.

Temmerman L. and Leschziner, M.A.(2001): "Large eddy simulation of separated flow in a streamwise periodic channel constriction", Proceedings, 2nd Symp. on Turbulence and Shear-Flow Phenomena, Stockholm.